positions allow coordination by O(31) and N(4), forming a 6-membered ring. Such a coordination model is not without precedence, having been observed in the crystal structure of ferrimycobactin P,[25] a linear dihydroxamate siderophore containing a single residue of *o*-hydroxyphenyloxazoline.

Upon examination of this coordination model,[22] it is apparent that a number of conformational changes occur in the ligand upon chelation. These include rotations (~180°) about bonds adjoining the tertiary amide carbonyl, N(3)–C(44) and C(44)–C(41), and about the bonds C(11)–C(17) and C(21)–C(27) to relieve the steric problems associated with close approach of O(13) and O(23) with the spermidine backbone. The butyl group undergoes a change from anti, anti, anti to gauche, anti, gauche conformations about the C(4)–C(5), C(5)–C(6), and C(6)–C(7) bonds, while the propyl arm remains gauche. Amide bonds I and II remain coplanar with 2,3-DHB groups 1 and 2; coplanarity of the oxazoline ring and 2,3-DHB 3 is retained, and the chelate is stabilized by at least one intramolecular hydrogen bond [O(41)–N(2)]. An alternative model[50] for metal coordination by agrobactin is the tricatecholate mode of chelation, made possible by the deprotonation of the meta catechol oxygen, O(32), and the transfer of the proton H(031) from the ortho oxygen, O(31), to the oxazoline nitrogen, N(4). The resulting ferric tricatecholate chelate remains dianionic at neutral pH with a proton count of five. This coordination model may possess less conformational strain in the spermidine backbone, with retention of coplanarity of the functionalities mentioned above. This mode of coordination is intriguing, although is not applicable to ferric chelation by the related linear ligand, parabactin.[22] Certainly, the coordination of ferric ion by agrobactin (and parabactin), the conformational changes occurring upon chelation, absolute configuration, and intramolecular contacts of these sequestering agents must be confirmed with solid-state studies, and experiments to this end have been initiated.

(50) The authors wish to thank one of the reviewers for his helpful comments.

Acknowledgment. We wish to express our appreciation to Professor J. B. Neilands for his generous gift of agrobactin and for his illuminating advice and discussions. One of us (D.L.E.-W.) wishes to thank Dr. M. B. Hossain for his help in collecting the intensity data. This research was sponsored by a grant from the National Institute of General Medical Science (GM-21822). We also wish to thank the University of Oklahoma Computer Center for providing computing services.

Supplementary Material Available: Listings of hydrogen atom coordinates and isotropic temperature factors, anisotropic thermal parameters of the nonhydrogen atoms, and structure amplitudes (30 pages). Ordering information is given on any current masthead page.

A Nuclear Magnetic Resonance Kinetic and Product Study of the Ring Opening of Propylene Oxide. Nucleophilic and General Catalysis by Phosphate[1]

Y. Pocker,* B. P. Ronald,[2] and L. Ferrin[3]

Contribution from the Department of Chemistry, University of Washington, Seattle, Washington 98195. *Received March 3, 1980*

Abstract: Systematic kinetic and product studies have been performed in an examination of the ring opening of propylene oxide over the entire pH region. The NMR kinetic method, which involves the integration of reactant and product resonances as a function of time, provided the rate data. The plots of log (area$_t$ – area$_\infty$) vs. time were linear to better than three half-life times of reaction. Reproducibility error for rate measurements run under identical conditions was less than 5%. Products were identified by ^{1}H and ^{13}C NMR spectroscopy and with gated decoupler techniques. The latter was used to quantitatively determine the product composition. The validity of this method of product analysis was carefully established with a series of control experiments. The error in these determinations was shown to be less than 4%. Emphasis was placed on the search for general and nucleophilic mechanisms of catalysis. Kinetic and product analyses were performed on reaction solutions in both aqueous formate and aqueous phosphate buffers. The glycol monoformate esters proved to be labile under kinetic conditions. By contrast the glycol monophosphate esters permitted a complete dissection of the buffer catalytic components into nucleophilic and general modes. Thus careful analysis of the reaction species present in the buffer matrix shows that glycol monophosphate esters are always produced in amounts less than the buffer contribution to the overall rate and furthermore arise almost exclusively from HPO_4^{2-} attack upon neutral epoxide. This nucleophilic catalysis accounts for 80 ■ 6% of $k_{HPO_4^{2-}}$ and leads to almost equal amounts of 1,2-propanediol-1-phosphate and 1,2-propanediol-2-phosphate. The remaining 20 ± 6% of $k_{HPO_4^{2-}}$ and the total $k_{H_2PO_4^-}$ represent general catalysis. These contributions arise mechanistically through hydrogen bonding which operates to increase the nucleophilic capacity of rear side water molecules or to enhance the electrophilic character of the epoxide ring, respectively.

During the past decade the properties of the epoxide linkage have been the subject of increasing interest in the realm of chemical and biochemical investigation. Special attention has focused upon two important investigative areas: the synthetic

(1) Support of this work by grants from the National Institutes of Health of the U.S. Public Health Service and the National Science Foundation is gratefully acknowledged. Part 5 of a continuing study devoted to the examination of the role of epoxides in vicinal diol dehydrations. Part 4: Y. Pocker and B. P. Ronald, *J. Am. Chem. Soc.*, **102**, 5311–5316 (1980). Part 3: Y. Pocker and B. P. Ronald, *J. Am. Chem. Soc.*, **100**, 3122–3127 (1978).

(2) Visiting Scholar in the Department of Chemistry, University of Washington, Seattle, Washington, while on sabbatical leave from the Department of Chemistry, Idaho State University, Pocatello, Idaho, from June 1978 through August 1979.

(3) National Science Foundation Undergraduate Research Participant during the period May through August 1977; Undergraduate Research Assistant, summer 1978.

0002-7863/80/1502-7725$01.00/0

utility and versatility of epoxides;[4a,b] and the biochemical roles played by these functional groups both as causative agents[5a,b] and as inhibitory agents[6] of mutagenesis and carcinogenesis. In both of these areas fundamental work has been done in attempting to relate the basis of biological activity to the mechanistic details of the chemical reaction.[7] A great deal of importance is thus attached to a thorough understanding of the mechanisms of epoxide ring opening and of the factors which exert influence in controlling the mechanistic pathway.

Among the first to recognize their unique reactivity was Brønsted, who initiated with Kilpatrick and Kilpatrick[8] a now classic study, demonstrating that three kinetically distinguishable components characterized heterolytic epoxide ring opening in aqueous media. Three decades later carefully refined and extended studies by Long and Pritchard,[9] using kinetics coupled with isotopic tracer techniques, supplied a mechanistic interpretation for the observed reaction velocity laws. A different mechanistic conclusion concerning epoxide ring-opening reactions was deduced by Whalley and co-workers[10] from measurements of the volume of activation for a selected series of epoxides. Parker and co-workers[11,12] reasoned that significant nucleophilic participation was necessary in the transition state to open the protonated epoxide ring. In all of these studies the observation of general catalysis proved elusive.

The application of the NMR kinetic method to the epoxide ring-opening problem led to the discovery of general acid catalysis concurrent with a nucleophilic acid catalyzed term for tetramethylethylene oxide.[1] Propylene oxide previously so well studied presented an area to test the method more thoroughly and to explore further the regiochemistry of nucleophilic reactions.

Formic acid buffer solutions were examined first but the nucleophilically generated formate esters (1- and 2-propane-1,2-diol formates) underwent facile hydrolytic decomposition. With phosphate buffers, however, this problem disappeared, and accurate kinetic and product data were acquired. Phosphate was selected because it was shown not to be nucleophilic toward epoxides in the elegant studies on arene oxide hydrolysis by Bruice et al.[7,13] Much to our surprise buffer incorporation into the products was found and was quite significant. This simple finding directs attention to the diversity of mechanistic features which operate in epoxide ring-opening chemistry.[11,14]

Experimental Section

Chemicals. Propylene oxide (Aldrich) was purified by distillation. The central fraction, boiling range 35–36 °C, was collected, redistilled twice, and stored in glass at −5 °C until required for study. The proton NMR spectrum in water, $CDCl_3$, and as a neat liquid showed the absence of impurities such as propionaldehyde and propylene glycol. The ^{13}C NMR spectrum failed to show evidence of polymeric material or propionaldehyde in the product derived from acid-catalyzed ring opening in the pH region 1–10. The UV spectrum of this epoxide dissolved in water showed only end absorption.

Propylene glycol (Aldrich) was used without further purification. Proton and ^{13}C NMR spectroscopy showed the absence of polymeric material and of propionaldehyde. Anhydrous formic acid, mp 8.25–8.35 °C, was derived from commercial formic acid (Eastman) as previously described.[1]

All salts were analytical reagent grade material and were dried for at least 24 h at 100 °C in a vacuum desiccator at 10^{-2} torr prior to use. Sodium perchlorate (Fischer Scientific) was dried as previously described.[1] A 2.0 M solution of the anhydrous salt in water had a pH of 6.8 at 25 °C.

Buffer solutions and standard solutions of acids and bases were prepared according to accepted analytical chemical procedures. Sodium perchlorate was used to control ionic strength at $\mu = 2.0$. Deuterium oxide of 99.8+% deuterium content obtained from Stohler Isotope Chemicals was used to make $DClO_4$ and NaOD solutions.

Kinetic Measurements. Kinetic studies were performed with a Varian Model T-60 nuclear magnetic resonance spectrometer, using the techniques described previously.[1] The resolution was maintained at between 0.8 and 1.0 Hz as measured by the width at half-height for the line of Me_4Si dissolved in $CDCl_3$. Special attention was given to the phase adjustment of the signal and to the integral drift control. These were optimized for each sample so that a flat base line was observed before and after each integral trace. Usually between 25 and 60 separate integrals were taken during the course of a given run. All reactions were followed for at least 3–4 half-lives unless product resonances obscured the epoxide signal. In this event a larger number of integral traces was recorded during the first half-life. Rate coefficients were determined graphically and by least-squares analysis of the integral data.[15] The plots provided a check on the least-squares analysis and served to detect curvature. In all cases linearity was very good, extending to better than 85% reaction. Calculations were performed on a PDP-8 laboratory minicomputer fitted with a CRT for visual analysis of data. Hard copy of the data and statistical and curve fitting results were printed on a Teletype.[16]

Product Studies. Products from all of the epoxide reactions were examined by both ^1H and ^{13}C NMR spectroscopy. Formate buffer systems produced very large quantities of formate esters as products of ring opening. In the case of phosphate buffer systems variable amounts of phosphate esters were produced depending upon the buffer ratio. The overlap of product resonances was extensive in the ^1H NMR spectra of both the formate and phosphate esters, and thus prohibited an unequivocal identification and quantitation. The chemical shift spread in the ^{13}C NMR spectrum facilitated both identification and analysis. Resonance assignment to the various monosubstituted formate esters was simplified by examination of esterification mixtures of propylene glycol in formic acid. The following assignments could be made:[17]

(4) (a) E. E. van Tamelen, *Acc. Chem. Res.*, **1**, 111–120 (1968); E. E. van Tamelen and D. R. James, *J. Am. Chem. Soc.*, **99**, 950–952 (1977); E. E. van Tamelen, A. D. Pedlar, E. Li, and D. R. James, *ibid.*, **99**, 6778–6780 (1977). (b) K. B. Sharpless and R. F. Lauer, *ibid.*, **95**, 2697–2699 (1973); G. H. Posner and D. Z. Rogers, *ibid.*, **99**, 8208–8218 (1977); R. K. Boeckman, Jr., K. J. Bruza, and G. R. Heinrich, *ibid.*, **100**, 7101–7103 (1978); P. C. Conrad and P. L. Fuchs, *ibid.*, **100**, 346–348 (1978); R. Huisgen, *Angew. Chem., Int. Ed. Engl.*, **16**, 572–585 (1977); W. E. Fristad, T. R. Baily, L. A. Paquette, R. Gleiter, and M. C. Bohn, *J. Am. Chem. Soc.*, **101**, 4420–4423 (1979).

(5) (a) D. L. Whalen, A. Ross, H. Yagi, J. M. Karle, and D. M. Jerina, *J. Am. Chem. Soc.*, **100**, 5218–5221 (1978); G. D. Berger, I. A. Smith, P. G. Seybold, and M. P. Serve *Tetrahedron Lett.*, 231–234 (1978). (b) D. M. Jerina and J. W. Daly, "Drug Metabolism—from Microbe to Man", D. V. Parke and R. L. Smith, Eds., Taylor and Francis, Ltd., London, 1976, pp 13–32; D. M. Jerina, R. E. Lehr, H. Yagi, O. Hernandez, P. Dansette, P. G. Wislocki, A. W. Wood, R. L. Chang, W. Levin, and A. H. Conney, "*In Vitro* Metabolic Activation in Mutagenesis Testing", F. J. deSerres, J. R. Fouts, J. R. Bend, and R. M. Philpot, Eds., Elsevier/North Holland Biomedical Press, Amsterdam, 1976, pp 159–176; J. W. Keller, N. G. Kundu, and C. Heidelberger, *J. Org. Chem.*, **41**, 3487–3489 (1976).

(6) S. M. Kupchan, Y. Shizuri, T. Murae, J. G. Sweeny, H. R. Haynes, M.-S. Shen, J. C. Barrick, R. F. Bruan, D. van der Helm, and K. K. Wu, *J. Am. Chem. Soc.*, **98**, 5719–5720 (1976); S. M. Kupchan, B. B. Jarvis, R. G. Dailey, Jr., W. Bright, R. F. Bryan, and Y. Shizuri, *ibid.*, **98**, 7092–7093 (1976).

(7) T. C. Bruice and P. Y. Bruice, *Acc. Chem. Res.*, **9**, 378–384 (1976); A. R. Becker, J. M. Janusz, D. Z. Rogers, and T. C. Bruice, *J. Am. Chem. Soc.*, **100**, 3244–3246 (1978); J. M. Janusz, A. R. Becker, and T. C. Bruice, *ibid.*, **100**, 8269–8271 (1978).

(8) J. N. Brønsted, Kilpatrick, and M. Kilpatrick, *J. Am. Chem. Soc.*, **51**, 428–461 (1929).

(9) F. A. Long and J. G. Pritchard, *J. Am. Chem. Soc.*, **78**, 2663–2667 (1956); J. G. Pritchard and F. A. Long, *ibid.*, **78**, 2667–2670, 6008–6013 (1956).

(10) E. Whalley, *Adv. Phys. Org. Chem.*, **2**, 93–162 (1964); J. Koskikallio and E. Whalley, *Trans. Faraday Soc.*, **55**, 815–823 (1959); *Can. J. Chem.*, **37**, 783–787 (1959).

(11) R. E. Parker and N. S. Issacs, *Chem. Rev.*, **59**, 737–799 (1959).

(12) J. K. Addy and R. E. Parker, *J. Chem. Soc.*, 915–921 (1963); J. K. Addy and R. E. Parker, *ibid.*, 644–649 (1965).

(13) D. Z. Rogers and T. C. Bruice, *J. Am. Chem. Soc.*, **101**, 4713–4719 (1979).

(14) J. G. Buchanan and H. Z. Sable, *Sel. Org. Transform.*, **2**, 1–95 (1972).

(15) Computations were performed on HP-25, HP-65, and HP-67 programmable pocket calculators by using a program generated for the purpose of least-squares standard error analysis. The program computes the least-squares slope, represent intercept, the standard deviation in both the slope and the intercept, and the correlation coefficient. All ± values after each quantity represent the standard deviation, σ, from the average. Division of σ by $n^{1/2}$, where n is the number of determinations, yields the standard error within the 68% confidence limit. J. Topping, "Errors of Observation and Their Treatment", 3rd ed., Chapman and Hall Ltd., London, 1962, pp 72–114. We thank Mr. T. Deits and Mr. D. Moore for sharing this program with us.

(16) Standard programs as described above (ref 15) were used with this computer facility. This facility and its ancilliary instrumentation represent the Masters thesis project of Mr. D. Moore in the Department of Electrical Engineering at the University of Washington.

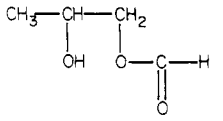

2-hydroxy-1-propyl formate, C(1) 68.1, C(2) 65.8, C(3) 17.6; and

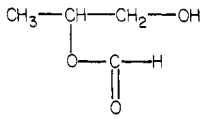

1-hydroxy-2-propyl formate, C(1) 64.1, C(2) 72.0, C(3) 14.9. The phosphate esters were easily identified through the two and three bond coupling between phosphorus and carbon, which persists under wide band proton noise decoupling. The assignment of resonances was done analogously for the formate system and is as follows:

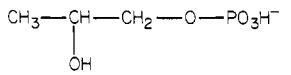

2-hydroxy-1-propyl phosphate, C(1) 70.5, C(2) 66.2, C(3) 18, $^2J_{COP}$ = 4.8 Hz, $^3J_{CCOP}$ = 6.6 Hz; and

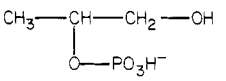

1-hydroxy-2-propyl phosphate, C(1) 70.5, C(2) 66.2, C(3) 18, $^2J_{COP}$ = 6.0 Hz, $^3J_{CCOP}$ = 7.8 Hz. Examination of the reaction mixtures in the UV showed the absence of chromophoric groups identifiable as carbonyl, thus precluding rearrangement processes in these studies. Indeed propylene oxide fails to produce detectable amounts of rearrangement products even in stronger acids (0.2 M H_3O^+) in the presence of 6 M $NaClO_4$.[19a]

Instrumental Methods. Proton nuclear magnetic resonance spectra for kinetic purposes and for product identification were obtained from a Varian Model T-60 nuclear magnetic resonance spectrometer. Carbon-13 NMR spectra were obtained from a Varian Model CFT-20 fourier transform nuclear magnetic resonance spectrometer. Routine spectra were obtained with standard parameters and proton noise modulated decoupling. Proton coupled spectra were obtained by using gated decoupling (decoupler off during acquisition) and a pulse delay of up to 5.0 s to provide time for NOE restoration. Spectra for integration were obtained similarly (decoupler on during acquisition only) and a pulse delay of 5–6 s was allowed for the decay of the NOE generated by the short decoupling period. Experiments with aqueous mixtures of propylene glycol and 1-propanol at four different concentrations showed that these parameter settings were appropriate for the integration of the hydroxyl bearing carbon resonances. Careful phasing of the signal was required to achieve an accuracy error of less than 4% for all of the standard samples. Spin–lattice relaxation measurements of propylene glycol in aqueous media yield $T_1(C_1)$ = 0.9 s, $T_1(C_2)$ = 1.57 s as the average values of four different determinations.[19b] Thus the 7–8 s duty cycle in the integral spectral measurements represents a compromise between reasonable instrument utilization time and quantitative accuracy. At the low concentrations (kinetic conditions) employed here upwards of 40 000 pulses are required to yield spectra with integrable signals above the noise.

Results

Propylene oxide, PO, in aqueous acidic or basic media undergoes ring opening to form exclusively propylene glycol, PG. No spectral evidence, either ^{13}C or ^1H NMR or UV, could be found for the formation of propionaldehyde by rearrangement or for the formation of di- or tripropylene glycol by polymerization processes.[20]

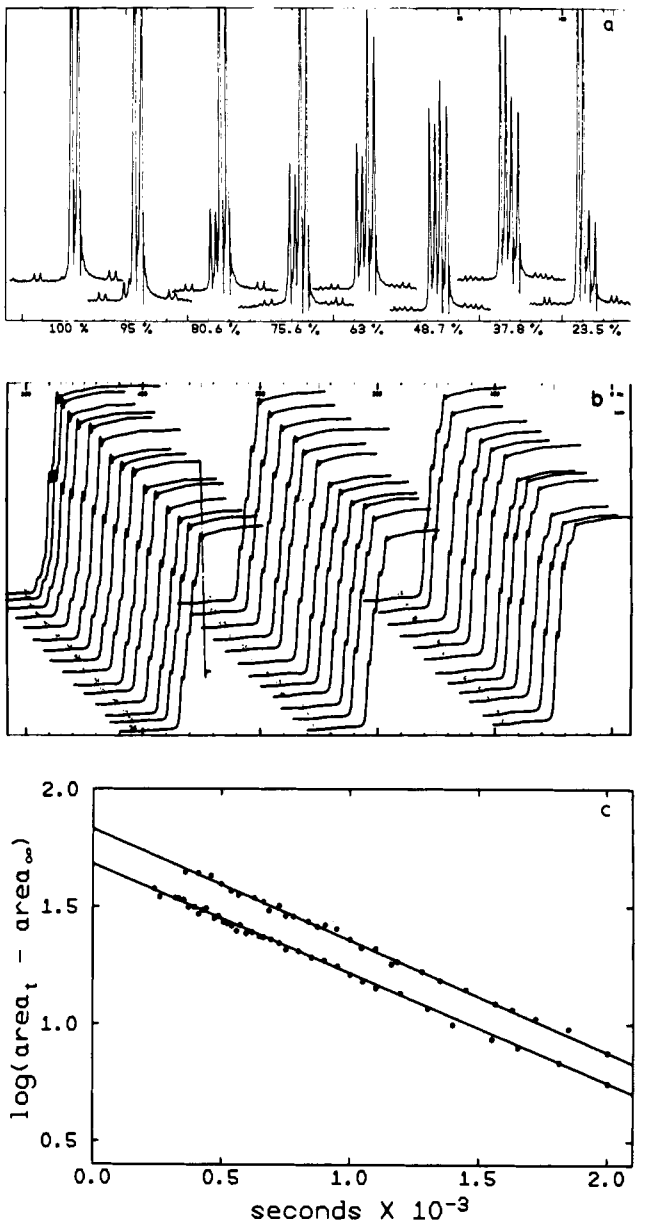

Figure 1. (a) Proton NMR spectra of the methyl region taken at various times during the course of hydration of propylene oxide. The low-field doublet corresponds to the methyl protons of the epoxide. The upfield doublet corresponds to the methyl protons of propylene glycol. The numbers at the bottom of each spectrum represent the percentage hydration of propylene oxide as calculated by measuring the integral step height for the epoxide doublet compared to the total integral step height. The reaction conditions were [PO] ≈ 0.8 M, pH = 2.4, and a temperature of 35 °C. The small resonances below and above the methyl signals are spinning side bands. (b) Repetitive timed integration curves taken during the course of propylene oxide hydration. The low-field resonances of the epoxide doublet are measured from the base of the peak to the maximum height. Clearly visible in the low-field and high-field portion of the trace are the spinning side bands. The conditions were pH = 2.1 ($HClO_4$), [PO] ≈ 0.9 M, and a temperature of 35 °C. (c) A plot of log (area$_t$ – area$_\infty$) vs. time for duplicate runs of the hydration of propylene oxide at pH 2.1 and a temperature of 35 °C. The reactions were followed to four or more half-lives. Linearity was excellent for three or more half-lives. Rate coefficients were calculated by the method of least squares and by graphical analysis and are (upper line) 1.09 ± 0.04 × 10^{-3} s^{-1} and (lower line) 1.07 ± 0.04 × 10^{-3} s^{-1}.

(17) These chemical shifts are approximate δ_c values corrected for external reference Me_4Si–$CDCl_3$. The important feature of these chemical shifts is not their absolute value but the differences which exist between them. The additivity of substituent chemical shift parameters coupled with the well-known pattern of carbon chemical shifts located α, β, or γ to a substitutent allow each resonance to be readily assigned.[18a,b]

(18) (a) J. B. Stothers, "Carbon-13 NMR Spectroscopy", Academic Press, New York, 1972, pp 55–310. (b) F. W. Wehrli and T. Wirthlin, "Interpretation of Carbon-13 NMR Spectra", Heyden and Sons, Ltd., London, 1978, pp 129–151.

(19) (a) Y. Pocker and B. P. Ronald, *J. Am. Chem. Soc.*, **102**, 5311–5316 (1980). (b) Relaxation time measurements were made by using the inversion recovery, (PD–180°–τ–90°–AT)$_n$ pulse sequence with a PD ≥ 20 s. Plots of log (peak height$_\infty$ – peak height$_\tau$) vs. τ were linear for $\tau \approx 2T_1$. Pulse widths were determined by standard methods.[18b]

(20) P. Ferrero, L. R. Flamme, and M. Fourey, *Ind. Chim. Belge*, **19**, 113–119 (1954). Data taken from this paper show that the extent of polymerization and dimerization is less than 0.2% in the mole fraction range ($M_{H_2O}/M_{PO} \approx$ 60–65) where kinetic studies were performed.

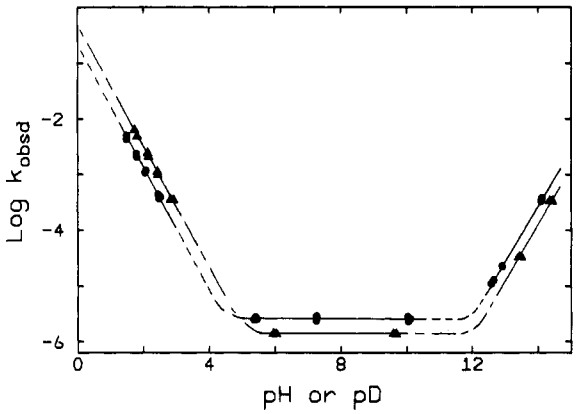

Figure 2. A plot of log k_{obsd} vs. pH or pD for the hydration of propylene oxide in both H_2O and D_2O media. The slope in the acidic, neutral, and basic limbs is respectively: ▲ (D_2O) −1.20 ± 0.04 and ● (H_2O) −1.07 ± 0.02, ☆ (D_2O) 0.00 and ● (H_2O) 0.00, ▲ (D_2O) 1.03 ± 0.01 and ● (H_2O) 1.00 ± 0.01. Each point represents the average of at least two rate coefficients from reaction followed as described above in Figure 1a–c (see text).

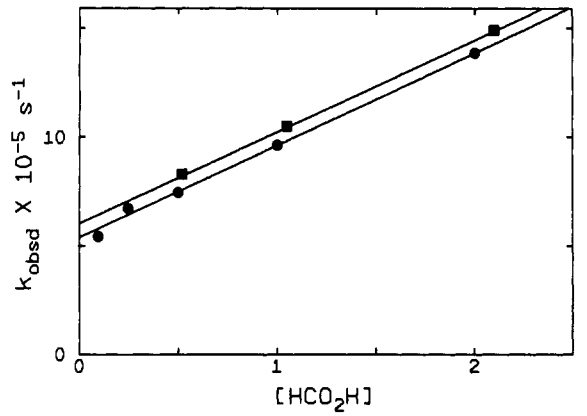

Figure 3. A Bell–Darwent plot (k_{obsd}, s^{-1} vs. the formic acid concentration) for propylene oxide hydration in formate buffers. Each point represents the average for two or more rate coefficients determined at constant pH, buffer ratio, and ionic strength, μ = 2.0. Inert salt when required was $NaClO_4$. Least-squares slopes are (■) 4.18 ± 0.09 × 10^{-5} M^{-1} s^{-1}, (●) 4.29 ± 0.20 × 10^{-5} M^{-1} s^{-1}. Least-squares intercepts yield from (■) $k_{H_3O^+}$ = 0.13 ± 0.01 M^{-1} s^{-1} and from (●) $k_{H_3O^+}$ = 0.14 ± 0.01 M^{-1} s^{-1}. The pH for (■) and (●) are respectively 3.32 and 3.45 at 35 °C.

The hydration process is conveniently followed by ^1H NMR spectroscopy, Figure 1a. The chemical shift difference between the downfield epoxide doublet and the upfield glycol doublet is 0.2 ppm (11–12 Hz). The lowfield resonance of the epoxide doublet is readily integrated as a function of time as shown in Figure 1b. The reaction yields first-order plots that are linear for over three half-lives with a correlation coefficient of 0.999 and a maximum reproducibility error of 4% between measurements made under identical conditions, Figure 1c. In a series of very dilute aqueous buffers, [total buffer] ≤ 10^{-3} M, the rate was observed to change with pH or pD as shown in a plot of log k_{obsd} against pH or pD, Figure 2. The three regions defined by this plot represent three distinct catalytic contributions to the overall rate equation and demonstrate how pH changes cause each term to become dominant. The least-squares slopes in the acidic limb are −1.07 ± 0.02 and −1.20 ± 0.04 in protiated and deuterated media, respectively, and thus confirm that the velocity in the acidic region is given by: velocity = $k_{H_3O^+}[H_3O^+][PO]$. Two independent methods have been used to evaluate $k_{H_3O^+}$. The first involves a least-squares extrapolation to zero pH or pD in Figure 2, while the second arises from the value of the intercepts in a Bell–Darwent[21] plot, Figure 3, derived from rate data in formate buffers,

(21) R. P. Bell and B. de B. Darwent, *Trans. Faraday Soc.*, **46**, 34–41 (1950).

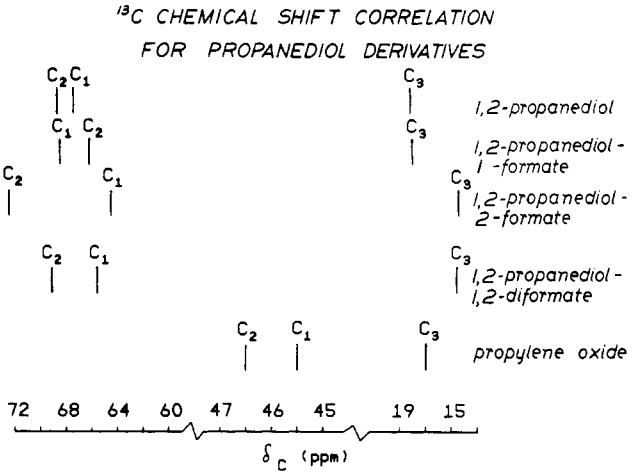

Figure 4. A ^{13}C chemical shift correlation chart for 1,2-propanediol, 1,2-propanediol–mono- and diformate esters, and propylene oxide. The chemical shifts are listed in the text corrected for external Me_4Si in $CDCl_3$.

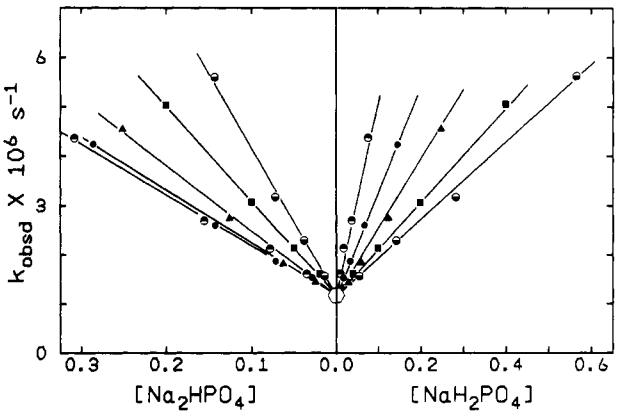

Figure 5. A Bell–Darwent plot (k_{obsd}, s^{-1} vs. the concentration) of components in various phosphate buffers of μ = 2.0 at 35 °C; left side, concentration of dihydrogen phosphate ion, right side, concentration of monohydrogen phosphate ion. The value of R, the buffer ratio, defined as [HPO_4^{2-}]/[$H_2PO_4^-$] for ⊖, ■, ▲, ●, and ⊖, is respectively 0.25, 0.50, 1.00, 2.00, and 4.00. Each point represents the data from duplicate rate runs at constant pH and buffer ratio as stated above. The least-squares treatment for each line provided a slope and a common intercept, which had a value of 1.13 ± 0.09 × 10^{-6} M^{-1} s^{-1}. The range of correlation coefficients was from 0.992 to 0.999.

Table I. Catalytic Rate Constants and Solvent Deuterium Isotope Effects

k, M^{-1} s^{-1}	isotope effect k_H/k_D
k_{H_2O} = 2.07 ± 0.10 × 10^{-8} [a]	
k_{H_2O} = 4.85 ± 0.31 × 10^{-8} [b]	1.80 ± 0.12
k_{H_2O} = 2.57 ± 0.05 × 10^{-8} [b]	
$k_{H_3O^+}$ = 1.4 ± 0.1 × 10^{-1} [a]	
$k_{H_3O^+}$ = 1.86 ± 0.17 × 10^{-1} [b]	0.33 ± 0.02
$k_{D_3O^+}$ = 5.49 ± 0.41 × 10^{-1} [b]	
k_{OH^-} = 2.99 ± 0.12 × 10^{-4} [b]	0.92 ± 0.07
k_{OD^-} = 3.26 ± 0.25 × 10^{-4} [b]	
k_{HCO_2H} = 4.24 ± 0.20 × 10^{-5} [a,c]	
$k_{H_2PO_4^-}$ = 5.33 ± 0.53 × 10^{-6} [a]	
$k_{HPO_4^{2-}}$ = 8.47 ± 0.26 × 10^{-6} [a,c]	
$k^{GEN}_{HPO_4^{2-}}$ = 1.75 ± 0.53 × 10^{-6} [a,d]	
$k^{NUC}_{HPO_4^{2-}}$ = 6.72 ± 0.47 × 10^{-6} [a]	

[a] Determined at μ = 2.0. The inert salt was $NaClO_4$. [b] Determined at μ = 1.0. [c] Gross rate coefficients not corrected for nucleophilic component. [d] Rate coefficients corrected for nucleophilic component.

Table I.

In the pH (pD) independent region the slope is zero. The spontaneous rate coefficient, k_0, being determined by two different

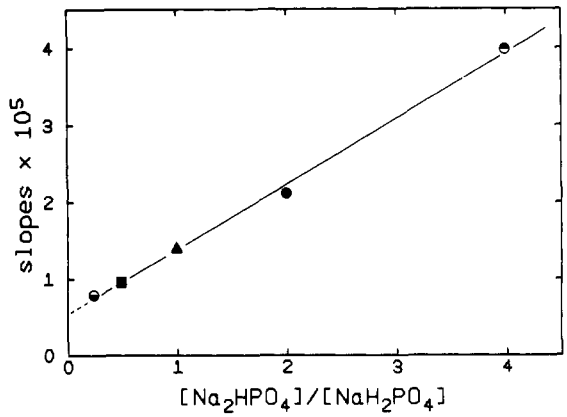

Figure 6. A plot of the slopes from the lines on the right side of Figure 5 against the buffer ratio, R. Least-squares treatment of the data yields a slope, $k_{HPO_4^{2-}} = (8.47 \pm 0.26) \times 10^{-6}$ M^{-1} s^{-1}, an intercept, $k_{H_2PO_4^-} = (5.33 \pm 0.53) \times 10^{-6}$ M^{-1} s^{-1}, and a correlation coefficient of 0.999. Identical results are obtained from the data on the left side of Figure 5.

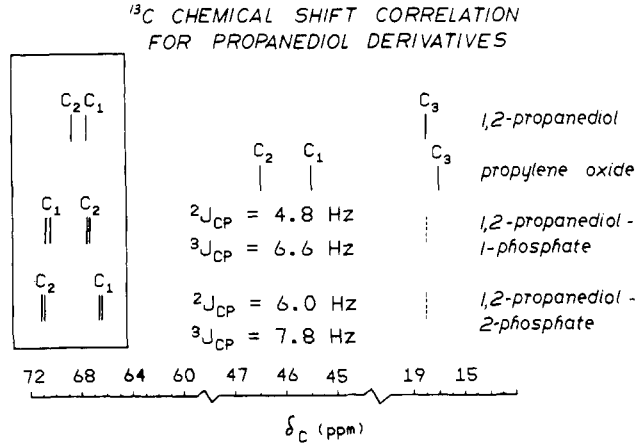

Figure 7. A ^{13}C chemical shift correlation chart for 1,2-propanediol, 1,2-propanediol-1- and -2-phosphate esters, and propylene oxide. The chemical shifts are corrected to external Me_4Si in $CDCl_3$. The two and three bond coupling constants were readily determined for the two phosphate esters. 1,2-Propanediol-1-phosphate: $^2J_{COP} = 4.8$ Hz, $^3J_{CCOP} = 6.6$ Hz, 1,2-propanediol-2-phosphate: $^2J_{COP} = 6.0$ Hz, $^3J_{CCOP} = 7.8$ Hz. The resonances in the boxed region were utilized for quantitative determination of products.

methods, direct determination and from Bell–Darwent plot intercepts, Table I (cf. also, Figure 5).

The rising limb in the high pH (pD) region gives rise to the velocity term: velocity = $k_{OH^-}[OH^-][PO]$. The slopes in H_2O and D_2O media are respectively 1.00 ± 0.01 and 1.03 ± 0.01. The values of k_{OH^-} and k_{OD^-} were derived from the observed rate in solutions of 0.96 M base, Table I.

Sufficient data in fully deuterated media were collected so as to determine the isotope effect k_H/k_D in each region of the profile. In the acidic region k_H/k_D has a value of 0.33 ± 0.02 which is suggestive of prior equilibrium protonation, although an H-bonded complex cannot be ruled out. The pH independent region isotope effect is $k_H/k_D = 1.80 \pm 0.12$. This can be accounted for by assuming that water of solvation assists in proton removal at the backside while participating in proton donation to the oxirane oxygen. The value of $k_H/k_D = 0.92 \pm 0.07$ in the basic region is indicative of nucleophilic participation by the base in the transition state for ring opening. This is fully in accord with the oxygen-18 labeling experiments of Long and Pritchard.[9]

In formate buffer systems at $\mu = 2.0$ it is possible to construct good Bell–Darwent plots, Figure 3. However, the rate increases are not due solely to general catalysis, since both ^1H and ^{13}C NMR spectra reveal that large amounts of formate esters are formed. Indeed ^{13}C NMR spectra of reaction mixtures of PO in formate buffers bear a strong resemblance to the spectra derived from propylene glycol–formic acid Fischer esterification mixtures. By studying the coupled and uncoupled ^{13}C spectra of various mixtures of propylene glycol and formic acid, and of water with propylene oxide and formic acid, it was possible to dissect the spectra as shown in Figure 4.[22] The ^{13}C chemical shifts of C(1) and C(2) in the ester products have a pedictable pattern.[17,18,22] The same pattern of resonances corresponding to both the 1- and 2-formate ester occurs when the products from PO ring opening in formate buffers are examined. However, both esters undergo hydrolysis sufficiently rapidly so that it is not possible to dissect the formic acid contribution to the rate into one term corresponding to general catalysis and the other to nucleophilic attack by formate ion on the protonated epoxide.[23]

During the course of determining the pH log–rate profile it was noticed that concentrated phosphate buffers, [buffer$_{total}$] = 2.0 M, caused observable rate changes as the buffer ratio was changed. A systematic study of catalytic effects in the pH-independent region showed that phosphate buffers catalyze the ring opening. Rate data acquired while following each reaction to over two half-lives[24] are shown in the form of a Bell–Darwent plot, Figure 5. Each point represents the average rate coefficient from two kinetic measurements at $\mu = 2.0$ and constant pH. Each line arises from a different buffer ratio, [basic form]/[acidic form], and has a correlation coefficient greater than 0.990 as calculated by least-squares treatment. The intercept common to the five lines is the value of k_0 which was confirmed by independent measurement of k_{obsd} at $\mu = 2.0$ in very dilute buffer in the pH independent region, vide supra. A plot of the slopes of the lines in Figure 5 against the buffer ratio yields a straight line whose least-squares slope is the catalytic coefficient for the basic form of the phosphate buffer and an intecept reflecting the catalytic coefficient for the acidic form, Figure 6. The correlation coefficient is 0.999. It is interesting to note that both forms of the buffer have catalytic contributions and that the basic form of the buffer, HPO_4^{2-}, has a coefficient 1.6 times larger than the acidic form. The larger kinetic term associated with the doubly charged form is apparently due to its greater nucleophilicity.

The development of additional resonances in the proton spectrum taken during the course of PO hydration in phosphate buffers substantiates the conclusion that a portion of the reaction rate arises from nucleophilic contributions. Indeed it has been known for some time that epoxides would react with phosphate buffers to yield alkyl monophosphate esters, though the yields are not especially good.[25] In previous synthetic studies only one of the phosphate esters was isolated and identified, although it was stated that the other ester was probably formed and was present. The

(22) Using gated decoupling techniques it was possible to establish the coupling pattern for each carbon atom in the ^{13}C NMR spectrum of the esterification mixture and for the reaction of propylene oxide with 100% formic acid. Since the glycol is the most abundant product in kinetic mixtures its resonances are most easily identified by their size and by spiking the reaction mixture with an authentic sample. Although the coupled resonances overlap the intensities would be predicted based upon the first order nature of >CH, $>CH_2$, $-CH_3$ coupled systems. Analysis of the intensities of the coupled system revealed the position of hidden resonances and allowed a complete assignment to be made to the decoupled spectrum.

(23) The pH region where rate data with formate buffers could be acquired ranged from pH 3.9 to 2.5. The formate esters generated by nucleophilic catalysis of propylene oxide ring opening in this region undergo an acid-catalyzed hydrolysis to propylene glycol. The rate of this pH-dependent hydrolysis is modestly rapid in the region of study. Crude estimates of the half-life time for these esters at pH = 3.3 are 12–14 h. The half-life time of the epoxide in this same medium is between 2 and 6 h, depending upon the formate buffer concentration. The relatively short lifetime of the esters coupled with the rather long time necessary for quantitative analysis by ^{13}C NMR makes it impossible to reliably assay these reaction mixtures.

(24) The half-life time for these phosphate catalyzed reactions in the pH-independent region ranged from 35 to 128 h.

(25) F. R. Atherton, H. T. Openshaw, and A. R. Todd, *J. Chem. Soc.*, 382–385 (1945); L. Kugel and M. Halmann, *J. Am. Chem. Soc.*, **88**, 3566–3572 (1966).

Scheme Ia

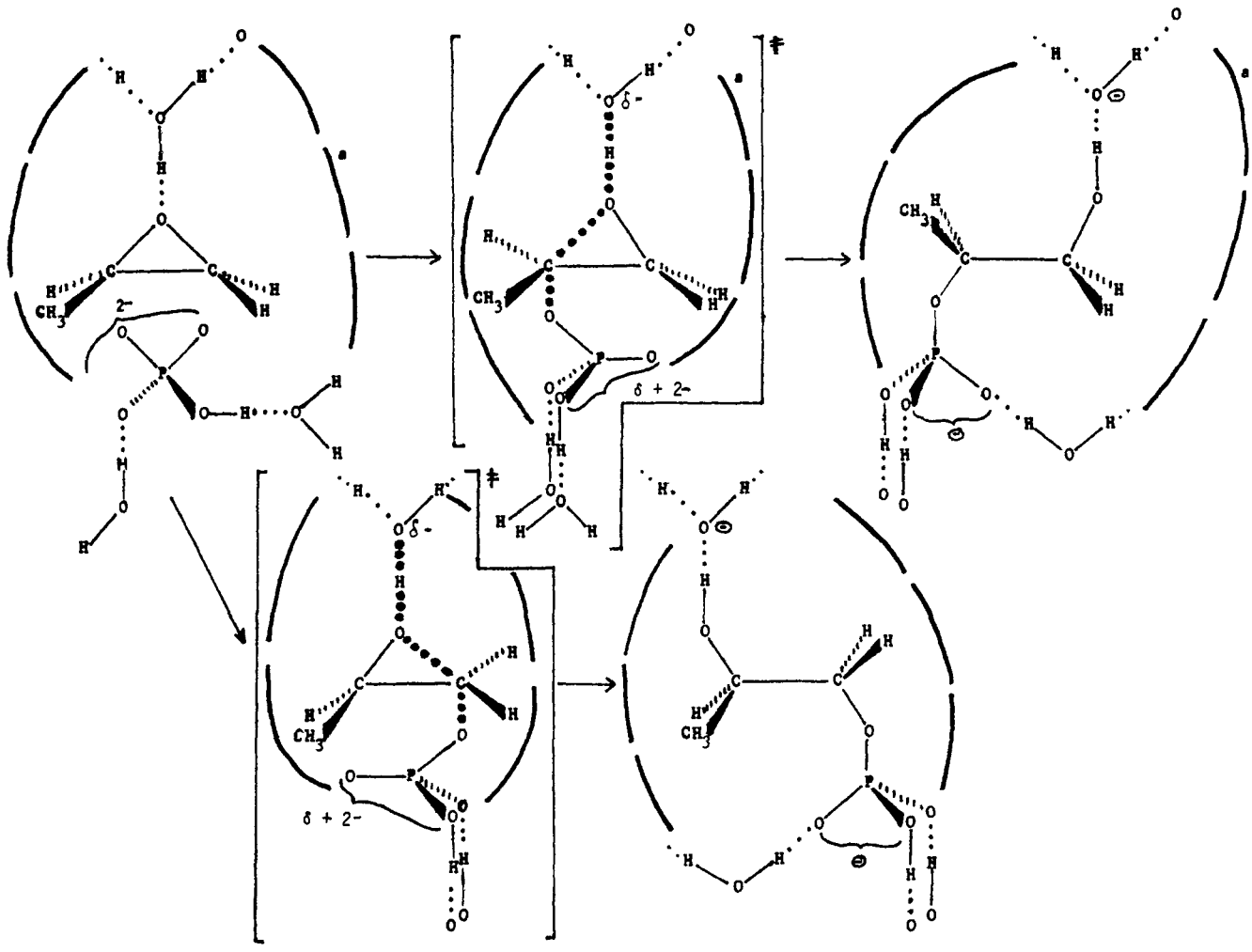

[a] The heavy dashed lines represent the remaining portion of the solvation sheath.

^{13}C NMR spectrum provides dramatic conformation of the fact that not one but two phosphate esters are formed, Figure 7.[26] The spectral features are not associated with the formation of polymeric material as has been demonstrated from spectra of the hydration of PO on the absence of phosphate buffers at the same pH.

Since the ^{13}C NMR spectrum readily revealed the presence of these esters and since the esters were found to be stable for long periods of time, conditions could be established for quantitation of a selected spectral region where uniquely separated resonances occurred. A comparison of the integral step height would provide the ratio of the esters and the fraction of total ester product. Such a unique spectral region is located where the C(1) and C(2) resonances occur for both the esters and the glycol, Figure 7. The separation between these several signals is quite adequate to allow estimation of the integrals. The appropriate ^{13}C NMR spectra were obtained by using gated decoupling with a pulse delay. This assured both the decay of the internuclear Overhauser enhancement and the full relaxation of the Z component of the magnetization prior to each pulse. The results in Table II indicate that the phosphate buffer system exhibits characteristics of both nucleophilic participation and general catalysis. This division into various catalytic contributions is possible because the total buffer rate component does not lead to a commensurate amount of buffer

Table II. Catalytic Contributions for Phosphate Buffers Reacting with Propylene Oxide at $\mu = 2.0$

buffer[a,b] ratio	$[Na_2HPO_4]$	$[NaH_2PO_4]$	% general[c,e] catal	% nucleophilic[d,e] catal
0.25	0.286	1.143	72.2	27.8
0.50	0.400	0.800	55.0	45.0
1.00	0.500	0.500	45.9	54.1
2.00	0.572	0.286	35.6	64.4
4.00	0.616	0.154	32.1	67.9

[a] Defined as [basic form]/[acidic form]. [b] The average pH derived from measurements of buffer solutions with the indicated ratio is respectively, 5.24, 5.67, 6.12, 6.49, 6.97. With substrate present the measured pH deviated by less than ±0.15 pH units from the listed values throughout the 20-fold serial dilution range. Rate coefficients were corrected for small changes in pH associated with buffer dilution. [c] Derived from the total buffer rate by correction for the amount of nucleophilic catalysis. This form of catalysis leads only to glycol. [d] Derived from a measurement of the products by ^{13}C NMR spectroscopy and by comparison to the total buffer rate. This form of catalysis leads only to phosphate mono esters. [e] Each value is based upon an average of between ten and fifteen integrals of the pertinent spectral region.

(26) The observed two and three bond coupling constants are completely in accord with values reported for other phosphate esters as shown below:[27]

phosphate ester	$^2J_{COP}$, Hz	$^3J_{CCOP}$, Hz
triallyl phosphate	5.2	7.0
tributyl phosphate	6.2	7.1
triphenyl phosphate	5.0	7.6
ATP^{2-}	4.7	8.8
ATP^{4-}	4.0	8.0

(27) L. F. Johnson and W. C. Jankowski, "Carbon-13 NMR Spectra: A Collection of Assigned, Coded, and Indexed Spectra", Wiley-Interscience, New York, 1972, pp 358, 353, 354, 451, and 477.

Scheme Ib

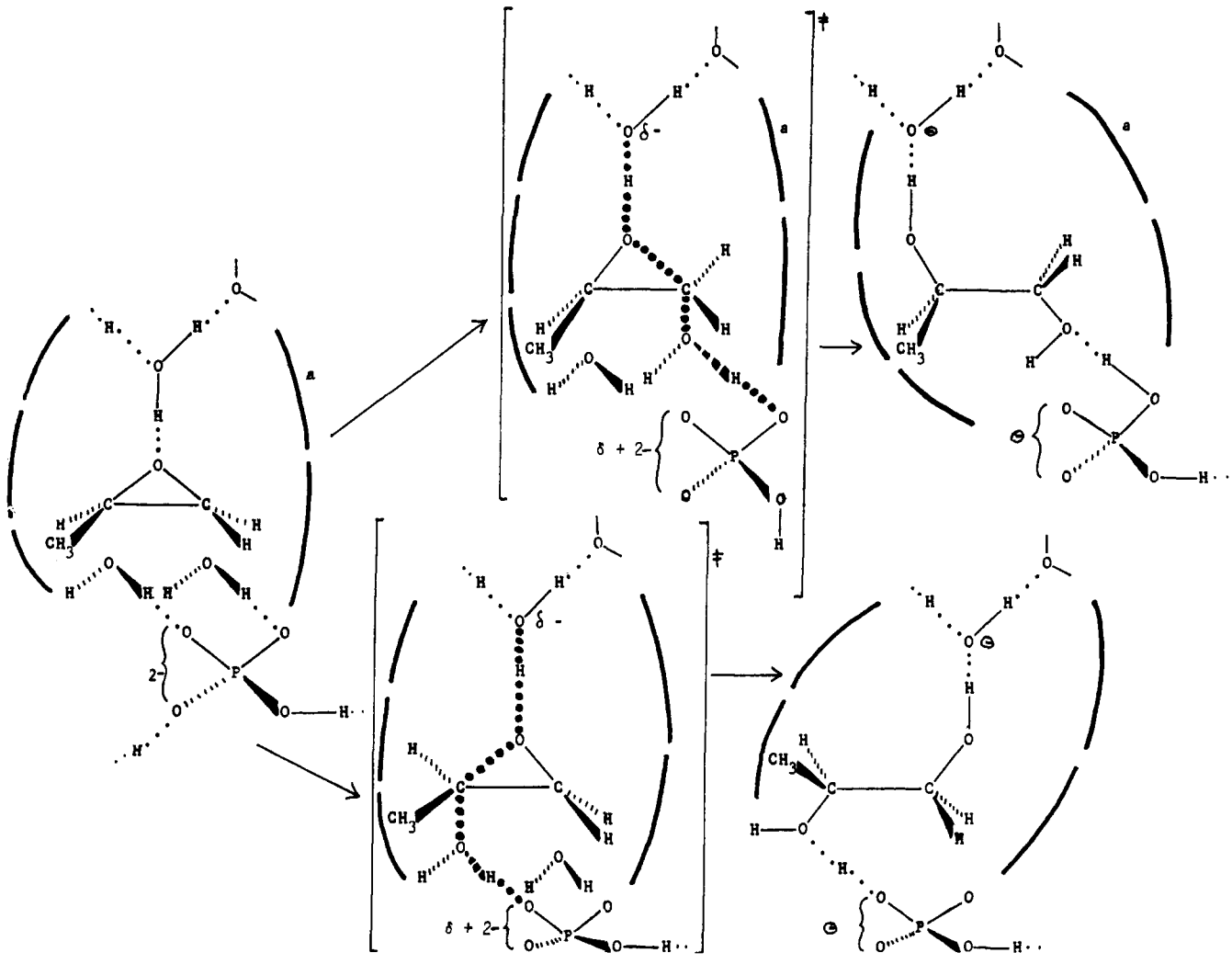

[a] The heavy dashed lines represent the remaining portion of the solvation sheath.

containing products,[28] and is independent of any mechanistic assumption. It is interesting to note that the ratio of the 1-phosphate ester to the 2-phosphate ester is 0.94 ± 0.17. Thus, the regiochemistry for the formation of these esters is quite different from that found for hydroxide ion or for water.[9] Furthermore the contributions to general catalysis by $H_2PO_4^-$ and HPO_4^{2-} are fully in accord with the observations made on many other substrates with phosphate buffer systems.

Discussion

The inflection points in Figure 2 indicate that different catalytic terms become dominant as a function of pH in the gross rate equation and thus subtle differences in reaction mechanism might apply to each pH region. The isotope effect, $k_H/k_D = 0.33 \pm 0.02$ for the acid-catalyzed limb, suggests that prior equilibrium protonation of propylene oxide might occur.[1,9] Thus an important intermediate, the protonated epoxide, would be generated. Its subsequent reaction is most interesting, for NMR and UV spectroscopic evidence seem to exclude the possibility for the existence of intermediates possessing the potential for skeletal rearrangement. Even when propylene oxide is ring opened in a 0.24 M $HClO_4$–6 M $NaClO_4$ solution there is no evidence of the formation of propionaldehyde.[19] The NMR spectra of mixtures of propylene glycol and propionaldehyde in 0.24 M $HClO_4$–6 M $NaClO_4$ solution indicate that these mixtures are stable both with respect to glycol rearrangement and to aldehyde isomerization. These facts suggest that the principal ring-opening pathway for the protonated epoxide is by nucleophilic assistance. Nucleophilically assisted ring opening would avert rearrangement and would, furthermore, be in accord with the sizable amounts of nucleophilically derived products that have been shown to be characteristic of this reaction. The transition state would thus possess considerable S_N2 character. Geometrical considerations tend to lend support to this view. The more spacious nature peculiar to the geometry of epoxides would allow for the greater

(28) The subdivision of each rate coefficient into nucleophilic and general components is based upon the following derivation.

$$\frac{\%\text{ general catalysis}}{\%\text{ nucleophilic catalysis}} = \frac{k^{GEN}_{H_2PO_4^-}[H_2PO_4^-] + k^{GEN}_{HPO_4^{2-}}[HPO_4^{2-}]}{k^{NUC}_{H_2PO_4^-}[H_2PO_4^-] + k^{NUC}_{HPO_4^{2-}}[HPO_4^{2-}]}$$

Following Table II assume that $k^{NUC}_{H_2PO_4^-}[H_2PO_4^-] \ll k^{NUC}_{HPO_4^{2-}}[HPO_4^{2-}]$, thus,

$$\frac{\%\text{ general catalysis}}{\%\text{ nucleophilic catalysis}} = \frac{k^{GEN}_{H_2PO_4^-}[H_2PO_4^-]}{k^{NUC}_{HPO_4^{2-}}[HPO_4^{2-}]} + \frac{k^{GEN}_{HPO_4^{2-}}}{k^{NUC}_{HPO_4^{2-}}}$$

Since $[H_2PO_4^-]/[HPO_4^{2-}] = 1/R$ where $R = [HPO_4^{2-}]/[H_2PO_4^-]$, thus

$$\frac{\%\text{ general catalysis}}{\%\text{ nucleophilic catalysis}} = \frac{k^{GEN}_{H_2PO_4^-}}{k^{NUC}_{HPO_4^{2-}}}\frac{1}{R} + \frac{k^{GEN}_{HPO_4^{2-}}}{k^{NUC}_{HPO_4^{2-}}}$$

A plot of (% general catalysis)/(% nucleophilic catalysis) vs. $1/R$ should be linear with an intercept of $k^{GEN}_{HPO_4^{2-}}/k^{NUC}_{HPO_4^{2-}}$. Since $k^{GEN}_{HPO_4^{2-}} + k^{NUC}_{HPO_4^{2-}} = k^{OBSD}_{HPO_4^{2-}}$ and $k^{GEN}_{H_2PO_4^-} \approx k^{TOTAL}_{H_2PO_4^-} = k^{OBSD}_{H_2PO_4^-}$ the fraction of $k^{OBSD}_{HPO_4^{2-}}$ attributed to general catalysis is easily computed. Treatment of the data in Tables I and II as described yields a straight line with correlation coefficient 0.993 and intercept 0.261 ± 0.079.

penetration of solvent molecules to the rear side of the oxirane carbon atoms.[10] Furthermore, this close approach of solvent molecules (or other species) to the back side would naturally provide the proper geometry (inversion of configuration) for a nucleophilic reaction.[4a,11]

The regiochemistry of the ring-opening step has been cited as the main argument supporting an S_N1 mechanism for this reaction. The ring opening, it is argued, causes a relief of ring strain and thus a reduction in the energy barrier leading to the transition state for carbonium ion formation. A consideration of the energy requirements of this mode of ring opening for each side of the oxirane linkage leads directly to the prediction that addition preferentially occurs to the most highly alkylated carbon atom.[9] This same ring-strain argument might well apply to a ring-opening process mediated by nucleophilic push. Indeed such a process may be quite facile since the substrate (protonated epoxide) would be very susceptible to the nucleophilic qualities of those proximate and properly placed solvent molecules.

There may exist a more fundamental and decisive explanation for the observed regiochemistry of acid-catalyzed ring opening through an analysis of orbital interactions. Observations such as differential regiochemistry with various nucleophiles would be in accord with this hypothesis.[11,29] The mechanism of the ring opening in the acid-catalyzed region would then be formulated as prior equilibrium protonation, followed by a nucleophilic attack by water, thus accounting for the solvent kinetic isotope effects and regiochemistry.

In the pH-independent region the solvent may play the role of a general-acid catalyst as well as a nucleophile. Through H bonding to the epoxide oxygen, water molecules thus help activate the oxirane system toward nucleophilic attack by other suitably located water molecules within the solvent shell. The magnitude of the rate coefficient for the spontaneous reaction in conjunction with diffusion controlled rate limitations prohibits this process from being formulated as hydroxide ion attack upon protonated epoxide.[30] The solvent kinetic isotope effect, $k_H/k_D = 1.80 \pm 0.12$, suggests that at least one proton must be transferred in the rate-determining step.

It is in the pH-independent region that phosphate buffers have been shown to play both a nucleophilic and general catalytic role. Greater nucleophilic character is to be expected in monohydrogen phosphate ion due to its greater charge density and increased number of nucleophilic sites. The experimentally observed regiochemistry of this nucleophilic addition indicates that attack on the primary and secondary centers occurs with almost equal probability, suggesting that steric factors may play only a minor role in determining the site of attack. Thus various nucleophilic species may possess intrinsically differential susceptibilities toward difunctional reaction centers which would lead to an observed nucleophile-specific regiochemistry. Scheme Ia illustrates the nucleophilic ring-opening process with monohydrogen phosphate ion. The small but significant general catalytic contribution (20 ± 6% of $k_{HPO_4^{2-}}$) associated with monohydrogen phosphate is described in Scheme Ib.[28]

The catalytic function of $H_2PO_4^-$ can be formulated in terms of two kinetically equivalent yet mechanistically distinct pathways, one involving general acid and the other specific acid–general base catalysis. A consideration of the microscopic reverse of these processes predisposes us toward the former pathway. Regardless of details, however, the $H_2PO_4^-$ ion is seen experimentally to play a singular role as a general catalyst.

Acknowledgment. We gratefully acknowledge a generous gift of high quality No. 505 Precision NMR tubes from the Norell Chemical Co. Inc., which facilitated this study. We also acknowledge the valuable assistance of Mr. B. J. Nist, University of Washington Spectroscopic Services Group, in obtaining ^{13}C NMR spectra for quantitative analytical purposes.

(29) M. J. S. Dewar and G. P. Ford, *J. Am. Chem. Soc.*, **101**, 783–791 (1979).

(30) Calculations show that k_0, the rate coefficient for the spontaneous reaction, considered for the case of hydroxide attack upon protonated epoxide in the pH independent region would exceed the diffusion limit. $k_{SPON} = k_0' K_a^{-1} [H_3O^+][OH^-]$ where $K_a^{-1} = [\text{epoxide}\cdot H^+]/\{[\text{epoxide}][H_3O^+]\}$. A value of $K_a^{-1} \approx 10^{-5}$ M^{-1} and $k_{SPON} = 1 \times 10^{-6}$ s^{-1} at pH = 7.0 leads to $k_0' \approx 10^{13}$ M^{-1} s^{-1}.[1,31]

(31) E. A. Moelwyn Hughes, "The Chemical Statics and Kinetics of Solutions", Academic Press, London, 1971, Chapter 5.